

ATTOSECOND TIMING

F. X. Kärtner, M. Xin, and K. Safak

Center for Free-Electron Laser Science, Deutsches Elektronen-Synchrotron and
 Physics Department and The Hamburg Center for Ultrafast Imaging, Universität Hamburg,
 Hamburg, Germany

Abstract

Photon-science facilities such as X-ray free-electron lasers (XFELs) and intense-laser facilities are emerging worldwide with some of them producing sub-fs X-ray pulses. These facilities are in need of a high-precision timing distribution system, which can synchronize various microwave and optical sub-sources across multi-km distances with attosecond precision. Here, we report on a synchronous laser-microwave network that permits attosecond precision across km-scale distances. This was achieved by developing new ultrafast timing metrology devices and carefully balancing the fiber nonlinearities and fundamental noise contributions in the system. New polarization-noise-suppressed balanced optical crosscorrelators and free-space-coupled balanced optical-microwave phase detectors for improved noise performance have been implemented. Residual second- and third-order dispersion in the fiber links are carefully compensated with additional dispersion-compensating fiber to suppress link-induced Gordon-Haus jitter and to minimize output pulse duration; the link power is stabilized to minimize the nonlinearity-induced jitter as well as to maximize the signal to noise ratio for locking.

Therefore, a multi-km attosecond-precision synchronization technique is imperative to unleash the full potential of these billion-dollar photon-science facilities.

The timing system consists of a reference providing extremely stable timing signals, a target signal that needs to be synchronized, a detector that can measure the timing difference between the target signal and the reference, and a control box to lock the timing of the target to that of the reference. If the target device is far away from the reference, a timing link is also necessary to deliver the timing signal from the reference to the target. Without exception, the attosecond-precision synchronization technique also requires these key elements.

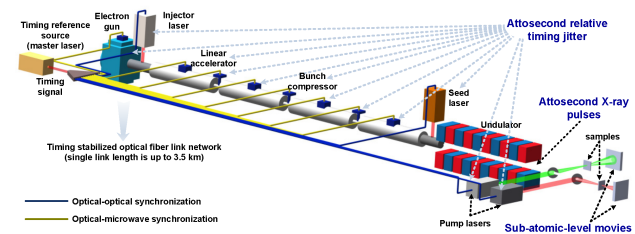


Figure 1: Timing and synchronization system for an attosecond XFEL [11].

INTRODUCTION

Recently, several X-ray FELs (XFELs), such as the European XFEL [1] in Hamburg, FERMI [2] in Italy, SwissFEL in Switzerland and Linac Coherent Light Source (LCLS) [3] and LCLS II [4] in Stanford and Dalian Coherent Light Source (DCLS) and SXFEL in China have been built and are in operation. The length of these facilities ranges from few hundred meters to several kilometers. Many of these facilities aim to generate attosecond X-ray pulses [5] with unprecedented brightness to film physical and chemical reactions with sub-atomic-level spatio-temporal resolution [6, 7]. Significant progress in attosecond science, including the time-domain observation of intramolecular charge transfer [8] and the discovery of ultrafast Auger processes altering the chemistry of matter on an attosecond time scale [9, 10], has been made in the past few years. Thus current XFELs technology will move over the next decade into the attosecond regime. As illustrated in Fig. 1, it is advantages to generate attosecond X-ray pulses and perform attosecond-precision pump-probe experiments. This is supported in an optimum way, if all optical/microwave sources in the XFEL, including the electron gun, injector laser, microwave references of the linear accelerator and bunch compressor, most importantly, the seed laser and pump lasers at the end station are synchronized simultaneously with attosecond relative timing jitter.

The timing reference source in attosecond synchronization can be an atomic clock [12, 13], a continuous-wave (CW) laser [14, 15] or a mode-locked laser [16, 17]. The state-of-the-art technique in each solution can provide an attosecond-jitter-equivalent instability for 1s observation time. In contrast to the other two solutions, a mode-locked laser can simultaneously provide ultralow-noise optical and microwave signals, and the ultrashort optical pulses in time domain can be directly used as time markers for precise timing measurements. So it is an ideal timing source for synchronization applications such as telescope arrays and XFELs, where the target devices are mode-locked lasers and microwave sources.

Another advantage of using mode-locked lasers is that it can provide very high sensitivity during timing detection, thanks to its high pulse peak power. For example, we have developed balanced optical cross-correlators (BOCs) [17, 18] and balanced optical-microwave phase detectors (BOMPDS) [19–21] for optical-optical and optical-microwave timing detection, respectively. Both of them can achieve attosecond precision and >1-ps dynamic range at the same time.

For remote synchronization, the timing link can be implemented as optical fiber link [22]. Optical-fiber-based timing

Content from this work may be used under the terms of the CC BY 3.0 licence (© 2018). Any distribution of this work must maintain attribution to the author(s), title of the work, publisher, and DOI.

links are very flexible for installation and can be easily fitted into XFELs and other facilities.

Here, we focus on the XFEL application, since it possesses currently the most urgent timing challenge. But the techniques we present here can also easily be adapted to other applications in the future. Based on the discussions above, the best synchronization solution for XFELs, as depicted in Fig. 1, should use a mode-locked laser (master laser) as the timing reference, and optical fiber links to distribute the timing signals to different remote laser/microwave sources. We have been working on this approach over the past decade [22, 23] and already passed the 10-fs precision level [24–26], which is more than an order-of-magnitude better than the best results achieved with traditional microwave signal distribution schemes. In order to meet the strict timing requirements of XFELs, a novel sub-fs-precision timing synchronization system is developed based upon our previous work, and presented here.

JITTER OF THE OPTICAL MASTER OSCILLATOR

Since the optical master oscillator (OMO) in Fig. 1 serves as timing reference for all optical/microwave sub-sources, it must exhibit attosecond-level timing jitter, which needs to be accurately characterized. Here, we use a balanced optical cross-correlator (BOC) [18, 23], which is intrinsically immune to AM-PM noise conversion by directly converting the timing difference of two optical pulses into a voltage signal. The BOC characterization has achieved extremely low noise floors down to 10^{-12} fs²/Hz for offset frequencies up to the Nyquist frequency of mode-locked lasers [26, 27].

The OMO jitter characterization setup is shown in Fig. 2. The output of two identical lasers (master and slave, with 216.667 MHz repetition rate, 50 mW average power, 170 fs pulse width and 1553 nm center wavelength) were combined by a polarization beam splitter (PBS) and launched into a BOC, which consists of a single 4-mm-long periodically-poled KTiOPO₄ (PPKTP) crystal operating in a double-pass configuration with appropriate dichroic beam splitter and mirror (DBS, DM) and a low-noise balanced photodetector (BPD). The BOC output was fed back to the piezoelectric transducer (PZT) of the slave laser (with a sensitivity of 17.4 Hz/V) through a proportional-integral (PI) controller so that the two lasers' repetition rates were locked to each other. Finally, the BOC output was sent to an SSA for jitter characterization.

It can be seen that as feedback gain increases, the low frequency jitter is suppressed below 50 kHz. So in terms of measurement, we can decrease the feedback gain as much as possible (e.g., to -20 dB), then we can obtain the accurate master-laser jitter between 1 kHz and 20 kHz and an upper limit estimate above this frequency range.

The master laser characterization results are displayed in Fig. 3. The top panel shows the jitter spectral density at different feedback gains. As predicted by the simulations, the jitter spectrum is limited by the detector noise floor (grey

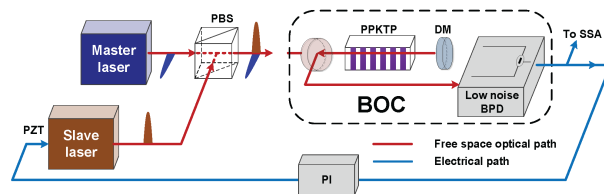


Figure 2: Master-laser (OMO) jitter characterization setup (PBS, polarization beam splitter; DBS, dichroic beam splitter; DM, dichroic mirror; PPKTP, periodically-poled KTiOPO₄; PI, proportional-integral controller; BPD, balanced photodetector; PZT, piezoelectric transducer; SSA, signal source analyzer).

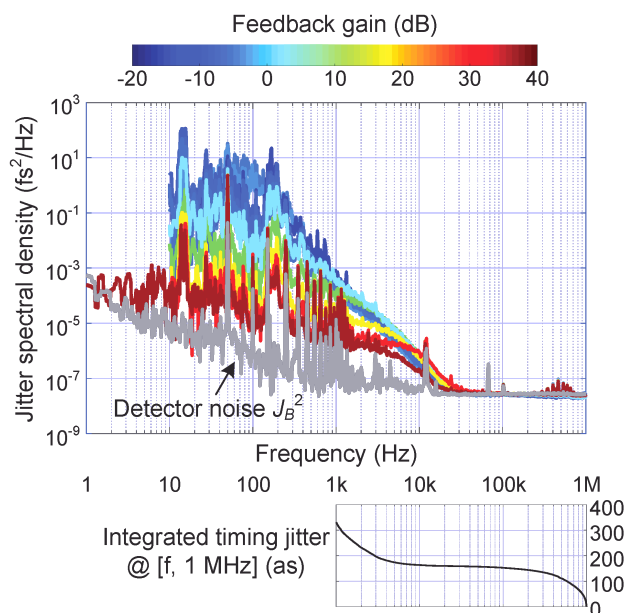


Figure 3: Measured master-laser jitter spectrum and corresponding integrated timing jitter [25].

curve) above 30 kHz. Between 1 kHz and 30 kHz, as the gain decreases, the spectrum approaches the real laser jitter. We choose the lowest gain value (about -15 dB) at which the locking is still stable enough to perform a measurement, and obtain 330 as integrated timing jitter from 1 kHz to 1 MHz, as shown in the bottom panel of Fig. 3. This value gives a very good upper limit estimate of the master laser's jitter. So this laser is definitely capable of providing the reference in an attosecondprecision timing synchronization system.

1550 nm LASER SYNCHRONIZATION

To test the local optical-optical synchronization an experimental setup shown in Fig. 4 is constructed. Similar to that in laser characterization, the repetition rates of the slave and master lasers were first locked together with an in-loop BOC, then another out-of-loop BOC was used to evaluate the jitter performance after synchronization. Both of the two BOCs have the same structure as that shown in Fig. 2. In the feedback loop, the output of the in-loop BOC was first filtered

by a PI controller. Then the PI output was separated into two paths: the first path was directly sent to the slave laser's PZT without amplification to compensate fast jitter above 10 Hz; the second path was sampled by a data acquisition (DAQ) card, analyzed by a Labview program to generate a DC voltage to compensate slow jitter below 10 Hz, and a voltage amplifier was used to extend the compensation range. This feedback design can effectively optimize the locking bandwidth and compensation range simultaneously.

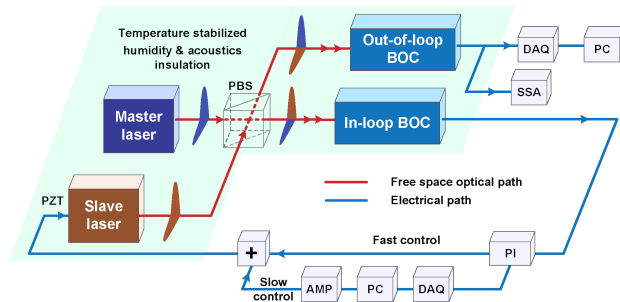


Figure 4: Local optical-optical synchronization (DAQ, data acquisition card; PC, computer, AMP, voltage amplifier; +, voltage summer).

To minimize the thermally-induced timing fluctuations, the two lasers, two BOCs and other free-space optics were mounted on a temperature-stabilized breadboard with a Super-Invar surface sheet. With temperature fluctuations controlled below ± 0.05 K, the effective timing instability of free-space beam paths due to thermal expansion is only ± 1 as/cm.

Figure 5(a) shows the out-of-loop jitter spectrum from 1 Hz to 1 MHz. The total integrated jitter over this frequency range is only 450 as. A long-term drift measurement was taken and the peak-to-peak drift in 10 hours is 400 as, which gives a root-mean-square (RMS) drift of 71 as (Fig. 6(b)). The Fourier transform of the drift data is also calculated in Fig. 6(c). The integrated drift from 200 μ Hz to 1 Hz is only 50 as. These results indicate that optical synchronization using BOC can easily achieve attosecond precision. Furthermore, they also provide a precision limit that we can approach in the remote timing synchronization.

SYNCHRONIZATION OF Ti:SAPPHIRE LASERS

In order to investigate the jitter noise limitations in the timing synchronization system, we built a Ti:Sapphire laser synchronization setup on a 4.7-km timing link network [28], as shown in Fig. 5. The same master laser as before was used, and its repetition rate was locked to an RF reference to reduce its drift below ~ 200 Hz. The slave laser, is a home-built Ti:Sapphire Kerr-lens mode-locked laser operating at 800-nm center wavelength and 1.0833 GHz repetition rate. Then the output of the master laser was split into two separate timing links. Timing link 1 consisted of a 3.5-km polarization-maintaining (PM) dispersion-compensated

fiber spool, a PM fiber stretcher, and a fiber-coupled motorized delay line with 560-ps range. Similarly, the components of timing link 2 included a 1.2-km PM fiber spool, a PM fiber stretcher, and a free-space motorized stage with 100-ps range. At the end of each link, there was a fiber-coupled mirror reflecting 10% of the optical power back to the link input. Here, a bidirectional erbium-doped fiber amplifier (EDFA) was also used to provide sufficient power for the backpropagating signal and the link output required for link stabilization and remote synchronization, respectively. At the link inputs, the round-trip pulses were combined with newly emitted ones in one-color (OC)-BOCs. OC-BOCs operate at 1554 nm wavelength and realize the crosscorrelation

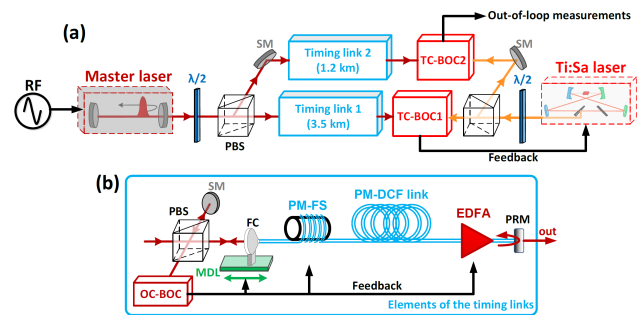


Figure 5: (a) Experimental setup for the synchronization of the Ti:Sa laser on a timing link network with a total length of 4.7 km. (b) Individual elements of the timing stabilized fiber links. Abbreviations: RF: RF reference; FC: fiber collimator; MDL: motorized delay line; PMFS: polarization-maintaining fiber stretcher; PM-DCF: PM dispersion-compensated fiber; EDFA: bidirectional erbium-doped fiber amplifier; PRM: partially reflecting fiber mirror [28].

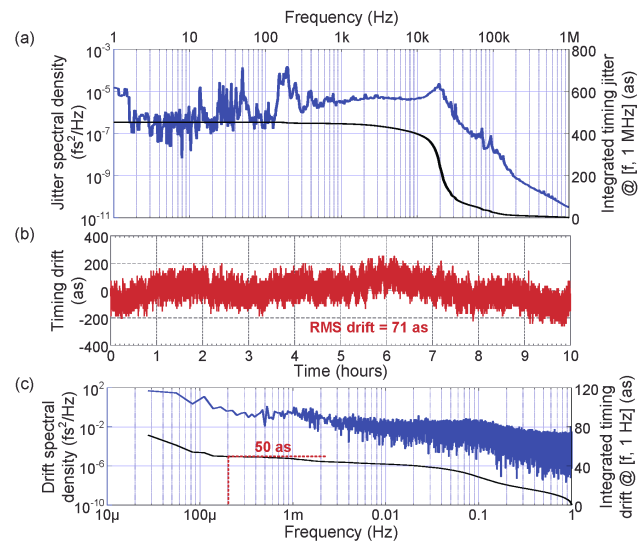


Figure 6: Local optical-optical synchronization measurement results. (a) Out-of-loop jitter spectrum; (b) long-term timing drift (sampling rate: 2 Hz); (c) timing drift spectrum.

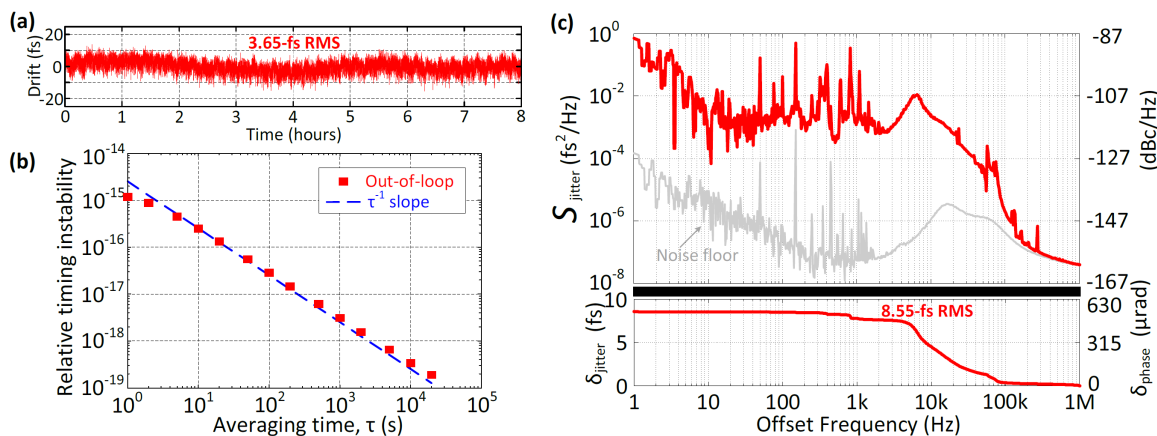


Figure 7: Out-of-loop measurements between the remotely synchronized Ti:Sa laser and timing link 2 output. (a) Timing drift below 1 Hz. (b) Calculated relative timing instability from the drift data. (c) Jitter spectral density S_{jitter} and its integrated jitter δ_{jitter} ; right axes: equivalent SSB phase noise $\mathcal{L}(f)$ and its integrated phase δ_{phase} scaled to a 10 GHz carrier frequency. The grey curve shows the noise floor of the free-running TC-BOC2 [28].

with the birefringence between two orthogonally polarized input pulses. OC-BOCs measured the propagation delay fluctuations in the links and generated error voltages, which controlled the fiber stretchers and the motorized delays to compensate for fast jitter and long-term drifts, respectively. The Ti:Sapphire laser was placed at the output location of the timing links. As the OMO and Ti:Sapphire laser operate at different central wavelengths, two two-color BOCs (TC-BOCs) [28] were built between each link output and the Ti:Sapphire laser output. Both of the TC-BOCs were realized with type-I sum-frequency generation between 800-nm and 1550-nm central wavelengths in a beta-barium borate (BBO) crystal. TC-BOC1 synchronized the Ti:Sa laser with link 1 output by tuning the repetition rate via its intracavity PZT mirror. Finally, the free-running TC-BOC2 evaluates the timing precision between the synchronized Ti:Sapphire laser and timing link 2 output.

Figure 7(a) shows the out-of-loop timing drift between the remotely synchronized Ti:Sa laser and timing link 2 output. We were able to keep the complete system synchronized for 8 hours continuously, which is limited by the PZT range of the Ti:Sa laser. The observed drift is only 25-fs peak-to-peak and 3.65 fs RMS for the complete duration without any excess locking volatility. We also calculated the relative timing instability (i.e., timing error in terms of overlapping Allan deviation) from the drift data to investigate the system behavior for different averaging times. As Fig. 7(b) illustrates, the relative timing instability is only 1.2×10^{-15} in 1-s averaging time (τ) and falls to 3.36×10^{-19} at 10,000 s following a deterministic slope very close to τ^{-1} .

The timing jitter spectral density for offset frequencies larger than 1 Hz was measured with a baseband analyzer, which Fourier transformed the TC-BOC2 output. The red curve in Fig. 7(c) shows the out-of-loop jitter between the remotely synchronized Ti:Sa laser and timing link 2 output. The integrated jitter for 1 Hz – 1 MHz is 8.55 fs RMS corre-

sponding to a phase error of 0.5 mrad for a 10 GHz carrier.

SUB-FEMTOSECOND PERFORMANCE

Demonstration of sub-femtosecond timing distribution was achieved with the laser-microwave network shown in Fig. 8a. The timing signal from the master laser is distributed through a network that contains two independent fiber links of 1.2-km and 3.5-km length operated in parallel. The link outputs are used to synchronize a remote

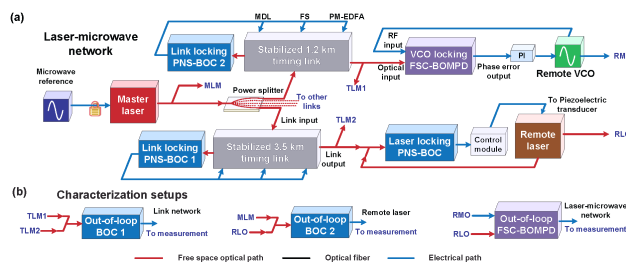


Figure 8: (a) Laser-microwave network (VCO, voltagecontrolled oscillator); (b) Out-of-loop characterization setups [11].

laser (e.g., serving as a pump-probe laser at the FEL end station) and a voltagecontrolled oscillator (VCO) (e.g., serving as a microwave reference of the FEL linear accelerator) simultaneously. New *polarization-noise-suppressed* BOCs (PNS-BOC) and *free-space-coupled balanced optical-microwave phase detectors* (FSC-BOMPDP) for improved noise performance have been and implemented. Residual second and third-order dispersion links are carefully compensated with additional dispersion-compensating fiber to suppress link-induced Gordon-Haus jitter and to minimize output pulse duration; the link power is stabilized to minimize the nonlinearity-induced jitter as well as to maximize the SNR for BOC locking. Characterization setups are shown

in Fig. 8b, to evaluate the performance of the link network, as shown in Fig. 9.

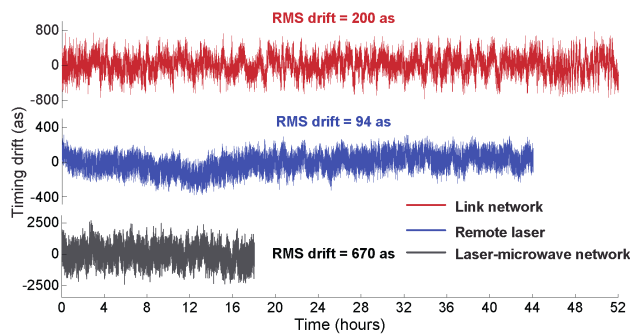


Figure 9: Measured long-term timing drift (sampling rate = 2 Hz).

The residual timing drift between links below 1 Hz is only 200 as RMS (red), and the total integrated timing jitter from 6 μ Hz to 1 MHz is 580 as (red). Remote laser synchronization over 44 hours without interruption is within 100 as RMS (blue). Overall, an unprecedented long-term precision of 670 as RMS out-of-loop drift over 18 hours (black) [11].

CONCLUSIONS

A sub-femtosecond laser-microwave network has been demonstrated with novel timing devices.

ACKNOWLEDGEMENT

This work was supported by the European Research Council under the European Union's Seventh Framework Program (FP/2007-2013) / ERC Grant Agreement No. 609920 and the Cluster of Excellence "The Hamburg Centre for Ultrafast Imaging—Structure, Dynamics and Control of Matter at the Atomic Scale" of the Deutsche Forschungsgemeinschaft.

REFERENCES

- [1] M. Altarelli, R. Brinkmann, M. Chergui, W. Decking, B. Dobsen, S. Düsterer, G. Grübel, W. Graeff, H. Graafsma, and J. Hajdu, "XFEL: The European X-Ray Free-Electron Laser", DESY, Technical Design Report, 2006.
- [2] E. Allaria *et al.*, "Highly coherent and stable pulses from the FERMI seeded free-electron laser in the extreme ultraviolet", *Nature Photon.* 6 (2012) 699.
- [3] P. Emma *et al.*, "First lasing and operation of an ångstrom-wavelength free-electron laser", *Nature Photon.* 4 (2010) 641.
- [4] J. Stohr, "Linac Coherent Light Source II (LCLS-II) Conceptual Design Report", SLAC, Design Report, No. SLAC-R-978, 2011.
- [5] E. Prat and S. Reiche, "Simple Method to Generate Terawatt-Attosecond X-Ray Free-Electron-Laser Pulses", *Phys. Rev. Lett.* 114 (2015) 244801.
- [6] C. Kupitz *et al.*, "Serial time-resolved crystallography of photosystem II using a femtosecond X-ray laser", *Nature* 513 (2014) 261.
- [7] H. Öström *et al.*, "Probing the transition state region in catalytic CO oxidation on Ru", *Science* 347 (2015) 978.
- [8] F. Calegari, D. Ayuso, A. Trabattani, L. Belshaw, S. De Camillis, S. Anumula, F. Frassetto, L. Poletto, A. Palacios, P. Decleva, J. B. Greenwood, F. Martín, and M. Nisoli, "Ultrafast electron dynamics in phenylalanine initiated by attosecond pulses", *Science* 346 (2014) 336.
- [9] S. K. Son, L. Young, and R. Santra, "Impact of hollow-atom formation on coherent x-ray scattering at high intensity", *Phys. Rev. A.* 83 (2011) 033402.
- [10] S. P. Hau-Riege, "Photoelectron dynamics in X-ray free-electron-laser diffractive imaging of biological samples", *Phys. Rev. Lett.* 108 (2012) 238101.
- [11] M. Xin, K. Şafak, M. Y. Peng, A. Kalaydzhyan, W. Wang, O. D. Mücke, and F. X. Kärtner, "Attosecond precision multi-km lasermicrowave network", *Light: Science & Applications* 6 (2017) e16187.
- [12] C. W. Chou, D. B. Hume, T. Rosenband, and D. J. Wineland, "Optical clocks and relativity", *Science* 329 (2010) 1630.
- [13] T. L. Nicholson, S. L. Campbell, R. B. Hutson, G. E. Marti, B. J. Bloom, R. L. McNally, W. Zhang, M. D. Barrett, M. S. Safronova, G. F. Strouse, W. L. Tew, and J. Ye, "Systematic evaluation of an atomic clock at 2×10^{-18} total uncertainty", *Nature Commun.* 6 (2015) 6896.
- [14] D. Meiser, J. Ye, D. R. Carlson, and M. J. Holland, "Prospects for a millihertz-linewidth laser", *Phys. Rev. Lett.* 102 (2009) 163601.
- [15] C. Hagemann, C. Grebing, C. Lisdat, S. Falke, T. Legero, U. Sterr, F. Riehle, M. J. Martin, and J. Ye, "Ultrastable laser with average fractional frequency drift rate below $5 \times 10^{-19}/s$ ", *Opt. Lett.* 39 (2014) 5102.
- [16] T. K. Kim, Y. Song, K. Jung, C. Kim, H. Kim, C. H. Nam, and J. Kim, "Sub-100-as timing jitter optical pulse trains from mode-locked Er-fiber lasers", *Opt. Lett.* 36 (2011) 4443.
- [17] A. J. Benedick, J. G. Fujimoto, and F. X. Kärtner, "Optical flywheels with attosecond jitter", *Nature Photon.* 6 (2012) 97.
- [18] T. R. Schibli, J. Kim, O. Kuzucu, J. T. Gopinath, S. N. Tandon, G. S. Petrich, L. A. Kolodziejski, J. G. Fujimoto, E. P. Ippen, and F. X. Kärtner, "Attosecond active synchronization of passively mode-locked lasers by balanced cross correlation", *Opt. Lett.* 28 (2003) 947.
- [19] J. Kim, J. Chen, Z. Zhang, F. N. C. Wong, F. X. Kärtner, F. Loehl, and H. Schlarb, "Long-term femtosecond timing link stabilization using a single-crystal balanced cross correlator", *Opt. Lett.* 32 (2007) 1044.
- [20] J. Kim, F. X. Kärtner, and F. Ludwig, "Balanced optical-microwave phase detectors for optoelectronic phase-locked loops", *Opt. Lett.* 31 (2006) 3659.
- [21] M. Y. Peng, A. Kalaydzhyan, and F. X. Kärtner, "Balanced optical-microwave phase detector for sub-femtosecond optical-RF synchronization", *Opt. Express* 22 (2014) 27102.
- [22] J. Kim, J. A. Cox, J. Chen, and F. X. Kärtner, "Drift-free femtosecond timing synchronization of remote optical and microwave sources", *Nature Photon.* 2 (2008) 733.

- Content from this work may be used under the terms of the CC BY 3.0 licence (© 2018). Any distribution of this work must maintain attribution to the author(s), title of the work, publisher, and DOI.
- [23] M. Y. Peng, P. T. Callahan, A. H. Nejadmalayeri, S. Valente, M. Xin, L. Grüner-Nielsen, E. M. Monberg, M. Yan, J. M. Fini, and F. X. Kärtner, “Long-term stable, sub-femtosecond timing distribution via a 1.2-km polarization-maintaining fiber link: approaching 10^{-21} link stability”, *Opt. Express* 21 (2013) 19982.
- [24] M. Xin, K. Şafak, M. Y. Peng, P. T. Callahan, and F. X. Kärtner, “One-femtosecond, long-term stable remote laser synchronization over a 3.5-km fiber link”, *Opt. Express* 22 (2014) 14904.
- [25] K. Şafak, M. Xin, P. T. Callahan, M. Y. Peng, and F. X. Kärtner, “All fiber-coupled, long-term stable timing distribution for free electron lasers with few-femtosecond jitter”, *Structural Dynamics* 2 (2015) 041715.
- [26] J. Kim, J. Chen, J. Cox, and F. X. Kärtner, “Attosecond-resolution timing jitter characterization of free-running mode-locked lasers”, *Opt. Lett.* 32 (2007) 3519.
- [27] J. A. Cox, A. H. Nejadmalayeri, J. Kim, and F. X. Kärtner, “Complete characterization of quantum-limited timing jitter in passively mode-locked fiber lasers”, *Opt. Lett.* 35 (2010) 3522.
- [28] K. Şafak, M. Xin, Q. Zhang, S. Chia, O. D. Mücke, and F. X. Kärtner, “Jitter analysis of timing-distribution and remote-laser synchronization systems”, *Opt. Express* 24 (2016) 21752.